WELDING RESEARCH

SUPPLEMENT TO THE *WELDING JOURNAL*, NOVEMBER 2000
Sponsored by the American Welding Society and the Welding Research Council

RESEARCH/DEVELOPMENT/RESEARCH/DEVELOPMENT/RESEARCH/DEVELOPMENT/RESEARCH/DEVELOPMENT

Oxygen Equivalent Effects on the Mechanical Properties of Titanium Welds

Understanding the effects of carbon, oxygen, nitrogen and cooling rate on weld properties will help in the development of a nondestructive test method for titanium

D. D. HARWIG, C. FOUNTAIN, W. ITTIWATTANA AND H. CASTNER

ABSTRACT. This investigation evaluated the use of an oxygen equivalent equation to predict the effects of the factors that control weld mechanical properties. These factors include solid-solution strengthening, grain size and microstructure. The latter two factors are related to the weld cooling rate below the beta transus. Full-penetration welds were made on commercially pure titanium and Ti-6Al-4V using argon-based shielding gases with small additions of either air or CO_2. These welds were made on sheet material using the autogenous GTAW process. Longitudinal weld metal tensile, macrohardness, microhardness, and interstitial composition specimens were removed from each weld. Bend tests also were performed to assess the effects of surface oxidation.

Weld color was shown to be a poor indicator of weld properties and only indicated some surface contamination occurred during solid-state cooling at high temperatures. Oxygen equivalent formulas and weld cooling rate were used to relate weld metal mechanical properties to weld alloy content. An oxygen equivalent formula (based on a formula developed by Ogden and Jaffee in 1955 for wrought alpha titanium alloys) was found to work well on weld metal for commercially pure (CP) titanium. An oxygen equivalent formula was developed for Ti-6Al-4V, but the relationship to weld properties did not relate strongly to variations in interstitial composition.

For CP titanium, Rockwell B hardness testing on the weld face can be used to correlate weld alloy content to mechanical properties, and may be used to assess welds for contamination.

D. D. HARWIG, W. ITTIWATTANA and H. CASTNER are with the Edison Welding Institute, Columbus, Ohio. C. FOUNTAIN is a former employee of the Edison Welding Institute.

KEY WORDS

Oxygen Equivalent Formulas
CP Tatanium
Ti-6Al-4V
GTAW
Interstitial Composition
Rockwell B Testing
Cooling Rate

Introduction

Contamination of titanium weld metal by interstitial elements (oxygen, nitrogen, carbon and hydrogen) reduces ductility and toughness, while increasing strength and hardness (Refs. 1–10). Contamination can be caused by poor cleaning of the joint and filler materials prior to welding, poor shielding of the weld zone or impurities in the shielding gas. Titanium forms a stable oxide layer that provides excellent corrosion resistance of the material at temperatures below 500°C (930°F) (Ref. 11). However, at temperatures above 500°C, the oxidation resistance of titanium decreases rapidly and the metal becomes susceptible to embrittlement by oxygen, nitrogen and hydrogen. The weld pool is the most vulnerable to contamination since diffusion of interstitial elements is very rapid in molten titanium. Contamination of the solidified weld bead or heat-affected zone (HAZ) usually only affects the material near the surface. Excessive contamination produces welds with poor properties. In addition, the high solubility of oxygen and nitrogen in titanium makes heating in air a problem. Heating titanium to high temperatures in air results not only in surface oxidation but also in solid-solution hardening as a result of inward diffusion of oxygen. The surface-hardened layer is known as alpha case. Because titanium oxide changes the color of the titanium surface, color is commonly used to visually inspect titanium components for contamination. Thick titanium oxide and alpha case layers must be removed before service because their presence reduces fatigue strength and ductility.

Accepted welding practice requires titanium welds to be bright and shiny with only slight discoloration. If normal practices are followed, the appearance of colors may indicate a problem with shielding equipment. Typically, welds that have colors of blue, purple or white are con-

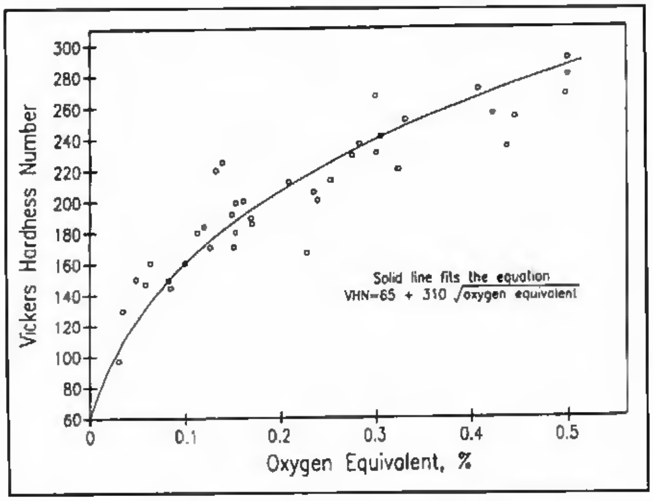

Fig. 1 — Effect of total interstitial content, expressed in terms of an oxygen equivalent, on the hardness of CP titanium base material (Ref. 10).

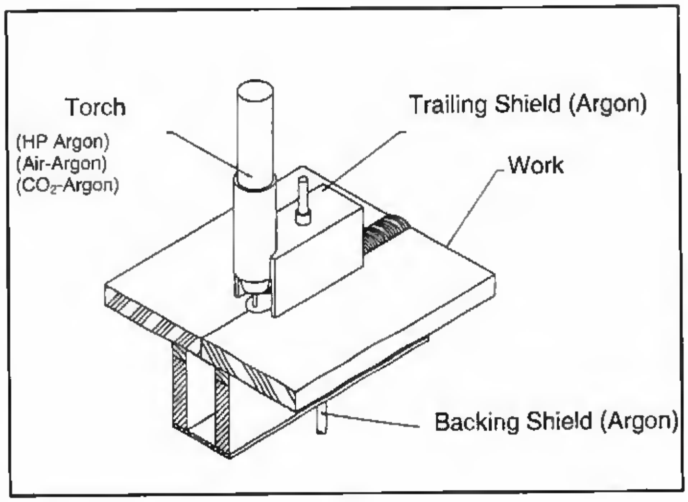

Fig. 2 — Setup for titanium weld tests.

sidered unacceptable and must be removed. Review of the literature reveals color is not always a reliable acceptance criteria (Ref. 8). Discoloration may only indicate the formation of an oxide on the surface of the weldment and may not directly relate to contamination that may have occurred in the molten weld pool. The bulk weld pool may have acceptable properties if the contamination occurred after solidification even though the titanium oxide may have unacceptable color. There is no currently acceptable method to determine if a discolored weld was properly shielded during solidification. Conversely, an unacceptable silver weld can be produced if a contaminated weld pool is well shielded after it solidifies since the surface oxide can dissolve into the subsurface.

The effect of welding procedure cleanliness on CP titanium weld properties has been characterized by numerous investigators (Refs. 3–9). In these investigations, titanium weldability was rated to be good due to solidification and solid-state cracking resistance with exceptional wetting, which promotes smooth weld beads. Solid-solution embrittlement of the HCP alpha phase by the interstitial elements carbon, nitrogen and oxygen was a primary source for manufacturing problems. Nitrogen is the most potent strengthener, followed by oxygen and carbon. Ogden and Jaffee determined nitrogen to have approximately twice the strengthening effect of oxygen (Ref. 10). An oxygen equivalent was formulated by these researchers to relate the effects of the interstitial elements on wrought CP titanium where

$$\text{oxygen equivalent, } OE_{CP} = (2/3 \times \text{wt-\% C}) + \text{wt-\% O} + (2 \times \text{wt-\% N}).$$

This equation was based on the properties of binary alloys and was used to relate the combined effects of the interstitial elements found in CP titanium to hardness — Fig. 1. Hydrogen and iron were not included in this formula because they are BCC beta phase stabilizers and have very low solubility in alpha-phase titanium. Hydrogen embrittles titanium by precipitation of hydride particles, which significantly lower impact strength (Refs. 4, 5, 11, 12). In CP titanium, 100 ppm (0.01 wt-%) of hydrogen has been reported to cause a loss of toughness and notch resistance but not to significantly affect strength and ductility. A small amount of beta (Ref. 13) (approximately 5%) is normally present in CP titanium from iron content and is believed to getter hydrogen and improve toughness (Ref. 12). Hydrogen is also believed to be responsible for porosity in titanium welds (Refs. 11,14). The effect of iron content on CP titanium welds was not reported.

Research data that relates titanium weld strength, hardness or ductility to an oxygen equivalent formula was not found. Several investigators (Refs. 6, 8, 9) reported titanium weld properties as a

Table 1 — Base Material Data

Ti Grade	Nitrogen Max (wt-%)	Carbon max (wt-%)	Oxygen max (wt-%)	Hydrogen max (wt-%)	Iron max (wt-%)	Ultimate stress min (ksi)	Yield min (ksi)	Elongation min (%)
Grade 1 (CP Ti)	0.03	0.08	0.18	0.015	0.20	35	25	24
Grade 2 (CP Ti)	0.03	0.08	0.25	0.015	0.30	50	40	20
Grade 3 (Cp Ti)	0.05	0.08	0.35	0.015	0.30	65	55	18
Grade 4 (CP Ti)	0.05	0.08	0.40	0.015	0.50	80	70	15
Grade 5 (Ti-6Al-4V)	0.05	0.08	0.20	0.015	0.40	130	120	10
Grade 23 (Ti-6Al-4V ELI)	0.03	0.08	0.13	0.0125	0.25	120	110	10
Heat No. 452141 0.079-in. (2-mm) thick, CP Ti	0.013	0.009	0.10	0.0010	0.06	69.1	46.2	27
Heat No. 420053 0.118-in. (3-mm) thick, CP Ti	0.007	0.01	0.15	0.0019	0.03	73.1	48.6	28
Heat No. 24-620 0.080-in. (2.03-mm) thick, Ti-6Al-4V	0.0091	0.013	0.16	0.0077	0.089	138	128	10
Heat No. W52H1B-RI 0.125-in. (3.17-mm) thick, Ti-6Al-4V	0.017	0.035	0.15	0.0054	0.19	148	140	19

function of contamination level introduced into their welding environment, such as dew point effects, but this data cannot be correlated to other welding applications. No oxygen equivalent equation has been found in the literature for the Ti-6Al-4V alloy (Refs. 15–29). In addition, the effects of weld cooling rate have not been related to alloy and interstitial content and weld properties. Titanium strength and hardness can be correlated to grain size and interstitial content using Hall-Petch relationships (Ref. 30). Weld cooling rate controls the grain size of the weldment. The effects of cooling rate need to be considered along with alloy and interstitial content to accurately predict the properties of titanium welds.

This investigation was initiated to improve the understanding of the effects of interstitial elements on the properties of welds in CP titanium Grade 2 and Ti-6Al-4V since these two alloys are the most commonly used in industry. Nondestructive testing of titanium welds for contamination is currently limited to visual examination of weld color. Many welds are repaired in industry based on weld color criteria since a better method does not exist. A future goal of industry is to develop nondestructive test methods to quantitatively evaluate the interstitial content (or contamination) of titanium welds. In a prior investigation (Ref. 1), the oxygen and nitrogen content of CP titanium welds was related to weld strength, hardness and ductility using the oxygen equivalent relationship developed by Ogden and Jaffee. This relationship was expanded in this investigation by evaluating the effects of carbon, oxygen, nitrogen and cooling rate on CP Grade 2 and Ti-6Al-4V alloy weld properties.

Experimental Procedure

Two thicknesses of CP titanium Grade 2 and two thicknesses of Ti-6Al-4V (Table 1) were used to make full-penetration bead-on-plate welds in the flat position. These welding tests used argon-based shielding gases that had controlled levels of either air or carbon dioxide (CO_2). For CP titanium, only air-argon mixtures were evaluated on the 0.079-in. (2-mm) material. Both air-argon and CO_2-argon shielding gases were evaluated on the other heats of material. The air-argon and CO_2-argon shielding gases were used to separately evaluate the effects of oxygen and nitrogen, and oxygen and carbon alloy additions. These shielding gases (Table 2) were only used in the welding torch so the interstitial elements would be absorbed primarily by the weld pool. Approximately 24 different shielding gas conditions were used for CP titanium and 20 different shielding gas conditions were used for Ti-6Al-4V, as shown in Table 3. This test matrix was developed to produce a range of weld metal compositions and cooling rates.

The gas tungsten arc welding (GTAW) process was used to make the test welds — Fig. 2. Most welds were made with a trailing shield attached to a No. 12 torch shield cup. Several welds were made just using shielding from either a No. 12 or No. 8 torch cup without a trailing shield. The inside diameters of the No. 12 and No. 8 cup were ¾ and ½ in. (19.05 and 12.7 mm), respectively. Twenty-four-inch (609.6-mm) long weld test coupons were sheared parallel to the rolling direction from each heat and thickness. The weld test coupon (Fig. 2) was clamped in a fixture that provided argon gas backing. Prior to welding each day, a 5 to 10 ft^3/h argon purge was applied for a minimum of 30 minutes and maintained between tests for both the torch and trailing shield. The titanium base metal was thoroughly cleaned using acetone and lint-free paper towels. Surface oxides were removed by wire brushing with a clean stainless steel wire brush, which was attached to an electric grinder and was only used on titanium. The weld joint area and weld fixture were wiped with acetone that was a minimum of 99.5% pure to remove wire brushing debris. An

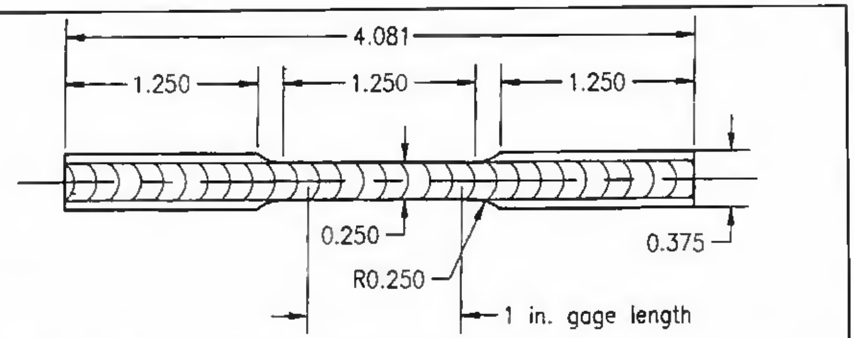

Longitudinal specimens shall be removed parallel and centered along the root bead surface

Fig. 3 — Longitudinal tension test specimen.

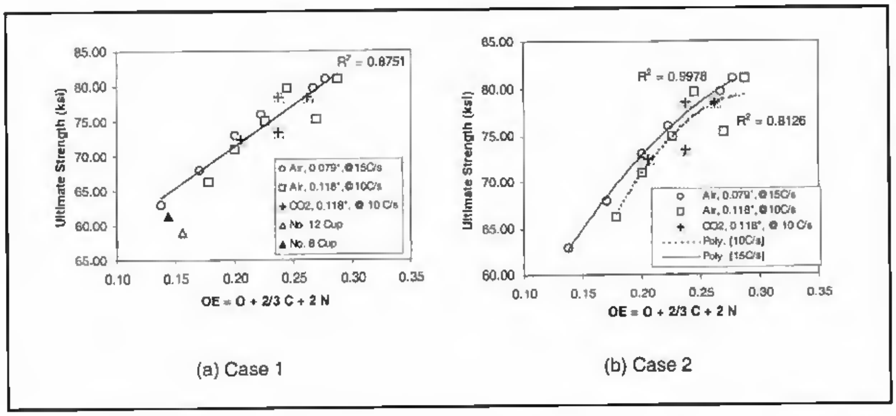

Fig. 4 — OE_{CP} effects on longitudinal ultimate strength.

Table 2 — Shielding Gas Test Conditions for GTA Welds

Torch Shield	Trailing Shield	Backing Shield
High-purity (HP) argon	Argon	Argon
High-purity argon w/no trail shield	—	Argon
Air-contaminated argon mixtures	Argon	Argon
–0.21% air		
–0.43% air		
–0.60% air		
–0.79% air		
–0.97% air		
CO_2-contaminated argon mixtures	Argon	Argon
–0.26% CO_2		
–0.52% CO_2		
–0.77% CO_2		
–1.00% CO_2		

Table 3 — Interstitial Composition Results for Autogenous Titanium and Ti-6Al-4V

Weld Condition	Test Condition	Avg C (wt-%)	Avg N_2 (wt-%)	Avg O_2 (wt-%)	Avg H_2 (wt-%)	Oxygen Equivalent
	HP-Argon	0.0205	0.014	0.115	0.00095	0.156
0.079 in. (2 mm)	0.21% Air	0.0205	0.028	0.12	0.0012	0.189
CP Ti	0.43% Air	0.023	0.0365	0.12	0.0011	0.208
Single pass	0.60% Air	0.0185	0.0555	0.11	0.00145	0.233
11°C/s cooling rate	0.79% Air	0.017	0.0625	0.125	0.00085	0.261
3.5 in./min TS	0.97% Air	0.0195	0.098	0.145	0.00085	0.354
	No. 12 cup	0.018	0.017	0.11	0.0010	0.156
	No. 8 cup	0.019	0.103	0.11	0.0011	0.149
	HP-Argon	0.018	0.0095	0.11	0.0007	0.141
0.079 in. (2 mm)	0.21% Air	0.022	0.021	0.12	0.0012	0.175
CP Ti	0.043% Air	0.020	0.033	0.12	0.0004	0.199
Single pass	0.60% Air	0.015	0.046	0.12	0.007	0.222
15°C/s cooling rate	0.79% Air	0.017	0.057	0.135	0.007	0.259
7.75 in./min TS	0.97% Air	0.021	0.061	0.145	0.008	0.278
	HP-Argon	0.011	0.0067	0.16	0.0018	0.181
0.118 in. (3 mm)	0.21% Air	0.011	0.015	0.165	0.0014	0.202
CP Ti	0.43% Air	0.012	0.021	0.175	0.0017	0.225
Single pass	0.60% Air	0.013	0.039	0.180	0.0016	0.265
10°C/s cooling rate	0.79% Air	0.010	0.055	0.170	0.0014	0.287
7.75 in./min TS	0.97% Air	0.015	0.051	0.175	0.0017	0.287
0.118 in. (3 mm)	0.26% CO_2	0.018	0.0068	0.18	0.0016	0.206
CP Ti	0.52% CO_2	0.031	0.0080	0.20	0.0012	0.237
Single pass	0.77% CO_2	0.032	0.0080	0.20	0.0015	0.237
10°C/s cooling rate	1.0% CO_2	0.039	0.0077	0.22	0.0004	0.261
7.75 in./min TS						
	HP-Argon	0.013	0.0110	0.16	0.0063	0.0001
0.080 in. (2.03 mm)	0.21% Air	0.020	0.0180	0.17	0.0053	0.2105
Ti-6Al-4V	0.43% Air	0.016	0.0300	0.17	0.0050	0.2205
Single pass	0.60% Air	0.018	0.0490	0.18	0.0060	0.4201
12.5°C/s cooling rate	0.79% Air	0.016	0.0590	0.19	0.0052	0.4663
9.0 in./min TS	0.97% Air	0.016	0.0810	0.19	0.0054	0.5775
0.080 in. (2.03 mm)	0.26% CO_2	0.024	0.0075	0.18	0.0053	0.2221
Ti-6Al-4V	0.52% CO_2	0.026	0.0068	0.18	0.0056	0.2583
Single pass	0.77% CO_2	0.042	0.0068	0.22	0.0050	0.6316
12.5°C/s cooling rate	1.0% CO_2	0.046	0.0022	0.24	0.0051	0.6992
	HP-Argon	0.046	0.0150	0.13	0.0036	0.1029
0.125 in. (3.17 mm)	0.21% Air	0.047	0.0330	0.14	0.0031	0.2738
Ti-6Al-4V	0.43% Air	0.050	0.0340	0.14	0.0028	0.3441
Single pass	0.60% Air	0.041	0.0590	0.14	0.0034	0.3512
11.8°C/s cooling rate	0.79% Air	0.047	0.0540	0.14	0.0031	0.4373
8.5 in./min TS	0.97% Air	0.039	0.0880	0.15	0.006	0.5452
0.125 in. (3.17 mm)	0.26% CO_2	0.049	0.0059	0.14	0.0039	0.1045
Ti-6Al-4V	0.52% CO_2	0.058	0.0085	0.16	0.0027	0.3323
Single pass	0.77%CO_2	0.060	0.0081	0.18	0.0029	0.3908
11.8°C/s cooling rate	1.0% CO_2	0.065	0.0086	0.19	0.0037	0.5089
8.5 in./min TS						

(a) $OE_{CP} = 2/3C + O + 2N$, $OE_{[illegible]} = 20.8C + 7.8N + 0 = 5.8Fe$
Test Temperature, 75°F.
Test condition was as-welded.

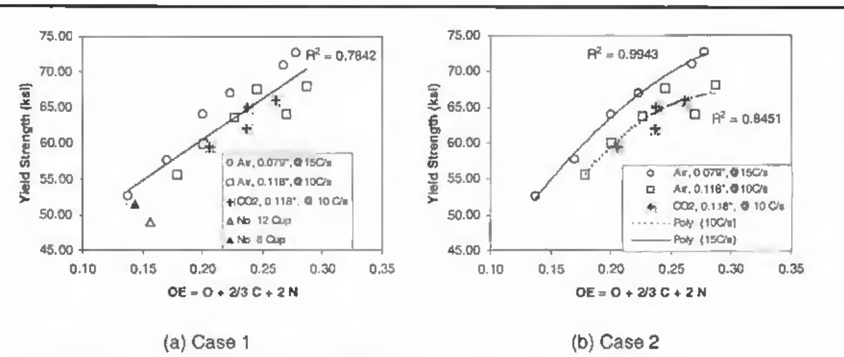

Fig. 5 — OE_{CP} effects on longitudinal yield strength.

argon backpurge was started in the backing chamber to provide at least a 20 to 1 dilution by volume before welding. The weld parameters developed for the autogenous welds used travel speeds from 3.5 to 9.0 in./min (1.48 to 3.81 mm/s) so that heat inputs would be typical of manual welding (Table 4). A minimum root bead width criteria of 0.25 in. (6.35 mm) was produced to permit the removal of all weld metal tensile specimens. Weld cooling rate was measured by immersing a tungsten-rhenium type C thermocouple that was 0.020-in. (0.5-mm) diameter into the weld pool. The cooling rate was determined between the temperature range of 500 to 800°C (1472 to 932°F). After welding, the weld assemblies were then sectioned into test specimens.

Three longitudinal weld metal tensile specimens were removed from each weld and the dimensions are shown in Fig. 3. Tensile specimens were tested in the as-welded condition where the face and root surface of the weld was as-welded (as-cast) and the edges of the flat tensile specimen were milled. The tensile tests were performed to ASTM E8 using a displacement rate of 0.05 in./min (0.02 mm/s). Specimens were also removed for microhardness testing, macrohardness testing, metallographic analysis and interstitial composition analysis. Microhardness and metallographic cross-sections were prepared by mounting the specimens in bakelite and polishing with up to 4000-grit sandpaper. A final polish was then performed using a colloidal silica suspension on an automatic cloth wheel. This step was repeated until all of the scratches were removed. The specimens were etched using a mixture of 88% distilled water, 10% hydrogen peroxide and 2% hydrofluoric acid. Composition of the welds was measured for interstitial elements oxygen, nitrogen and carbon using the ASTM E-1019 combustion method. Hydrogen was measured using the ASTM E-1447MOD combustion method. Vickers microhardness measurements were taken using a load of 500 g for 15 s on a mounted cross section. An average Vickers microhardness was calculated from nine measurements. All measurements were made in the fusion zone and were intragranular. Rockwell macrohardness measurements were made on the surfaces of the welds in the fusion zone, HAZ and base metal.

Tensile strength, ductility and hardness data were plotted as a function of oxygen equivalent. Statistical analysis was used to best fit the relationship between that property and the oxygen equivalent equation. For CP titanium, the data fit was analyzed for two cases:

1) A direct relationship between that property and OE.

2) An indirect relationship between that property and OE as a function of cooling rate.

The coefficient of multiple determination was calculated for each data fit for both cases. In the case of Ti-6AL-4V, a complete regression analysis was performed to derive a new oxygen equivalent equation that maximized the relationship between Ti-6Al-4V weld properties and alloy content.

Regression Analysis for Ti-6Al-4V OE

The objective of the regression analysis was to find the best relationships between mechanical properties and the oxygen equivalent. To reach this objective, regression analysis must find the best fit of oxygen equivalent coefficients and minimize the total error estimation. The approach was as follows:

First, an oxygen equivalent was established by parameterizing the coefficients of the chemical compositions. This oxygen equivalent was fit to each of the mechanical properties using the least-squared error method. The average R-squared value was then calculated and minimized over the parameterized chemical composition coefficients to guarantee a best fit. This procedure is summarized by the following equations:

Let A_i = chemical compositions of run i $= [a_{1i}\ a_{2i} \dots a_{r,i}]^T$. That is $A_i = [\%C_i\ \%N_i\ \%O_i\ \%Fe_i]^T$.

C = chemical composition coefficients $= [c_1\ c_2 \dots c_r]$.

z_i = oxygen equivalent of run i $= CA_i$, i = 1,..., n.

$Z = [Z_1\ Z_2\ \dots\ Z_n]^T$ That is $z_i = c_1{*}(\%C)_i + c_2{*}(\%N)_i + c_3{*}(\%O)_i + c_4{*}(\%Fe)_i$.

x_{ij} = design matrix, i = 1,...,n, j = 1,...,p-1.

$$X = \begin{bmatrix} 1 & x_{11} & x_{12} \\ 1 & x_{21} & x_{22} \\ M & x_{ij} & M \\ 1 & x_{n1} & x_{n2} \end{bmatrix}$$

$$= \left[1\ \ Z\ \ Z^2\right] = \begin{bmatrix} 1 & Z_1 & Z_1^2 \\ 1 & Z_2 & Z_2^2 \\ M & & \\ 1 & Z_n & Z_n^2 \end{bmatrix}.$$

y_{ik} = mechanical property (response) k from run i = 1,..., n, k = 1,..., m.
$Y_k = [y_{1k}\ y_{2k} \dots y_{nk}]^T$, k = 1,..., m.

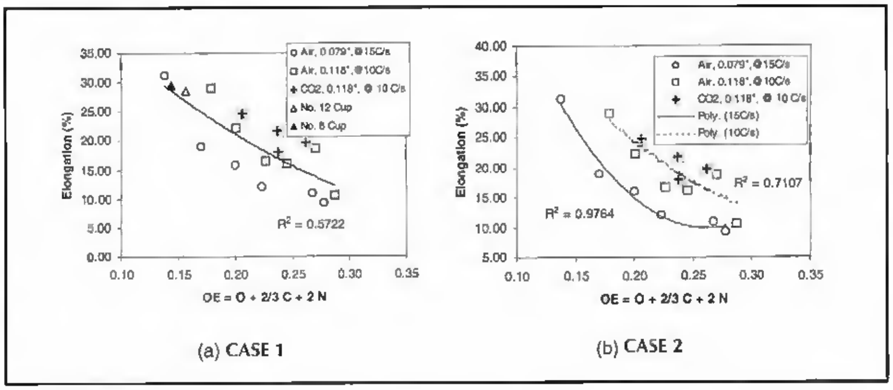

Fig. 6 — OE_{CP} effects on longitudinal tensile elongation.

Table 4 — Autogenous Welding Parameters

Thickness (in.)	Weld Condition	Current (amps)	Voltage (volts)	Travel Speed in./min	mm/s	Cooling Rates (°C/s)
0.079 (2.0 mm) CP Ti	single pass (autogenous)	70	8.0	3.5	1.48	11
0.079 (2.0 mm) CP Ti	single pass (autogenous)	120	9.0	7.75	3.28	15
0.118 (3.0 mm) CP Ti	single pass (autogenous)	200	10.0	7.75	3.28	10
0.080 (2.03 mm) Ti-6Al-4V	single pass (autogenous)	125	13.0	9.0	3.80	12.5
0.125 (3.17 mm) Ti-6Al-4V	single pass (autogenous)	225	11	8.5	3.60	11.8

The model used was $Y_k = X B_k + \varepsilon_k$, k = 1,..., m, where $B_k = [ß_{0k}\ ß_{1k}\ ß_{2k}]$, k = 1,..., m, and $ß_{jk}$ was the regression coefficient. The error term ε in the model was assumed to have E(ε) = 0 and V(ε) = σ^2, and the $\{\varepsilon_i\}$ were uncorrelated random variables. Let L represent the sum of the squared errors, ε_{ik}, $y_{ik} - \hat{y}_{ik}$, where $\hat{y}_{ik}$ was the estimated y_{ik}, $\varepsilon_{ik} = y_{ik} - \hat{y}_{ik}$, i = 1,...,n, k = 1,...,m, or $\varepsilon_k = [\varepsilon_{1k}\ \varepsilon_{2k} \dots \varepsilon_{nk}]^T$.

$$L = \sum_{k=1}^{m}\sum_{i=1}^{n}\left(y_{ik} - \left(\beta_{0k} + \sum \beta_{jk}x_{ijk}\right)\right)^2$$
$$= \sum_{k=1}^{m}\left(Y_k'Y_k - 2B_k'X'Y_k + B_k'X'XB_k\right).$$

The least squares method takes the partial differential of L with respect to $ß_{jk}$, j = 0,1,2, k = 1,..., m, and set it to zero. Solving the least square normal equations derived the coefficient $ß_{jk}$, which minimizes the sum of the squared errors.

$$\left.\frac{\partial L}{\partial B}\right|_{\hat{\beta}_k} = 0 \text{ or } -2X'Y_k + 2X'X\hat{B}_k = 0, k = 1,\dots,m.$$

Solving the normal equations above derived the regression coefficients $\hat{\beta}_k$, the relationship of mechanical properties to the oxygen-equivalent equation,

$\hat{\beta}_k = (X'X)^{-1}X'Y$. The estimated y_{ik} for the fitted regression model was

$$\hat{Y}_k = X\hat{B}_k.$$

Further, the residual sum of squares (SS_E), the regression sum of squares (SS_R) and the total sum of squares (SS_T) were estimated to identify the coefficient of multiple determination R^2 and the adjusted R^2 for each relationship of X and Y_k per the definitions as defined in Design and Analysis of Experiments (Ref. 31).

The chemical coefficient matrix C was estimated such that it gave the least squared error fit to each of the regression coefficients $\hat{B}_k$. Thus, nonlinear programming was used to maximize the total $R^2_{adj,k}$, which indicates how good the fits were taking into account the number of variables and the number of runs (n) in each Y_k. The formulation of the nonlinear program was as follows:

$$\max_{C} \sum_{k=1}^{m} R^2_{adj,k}$$

Subject to $c_3 = 1$.

The only constraint was set to prevent multiple sets of solutions that would give

Table 5 — Color of Titanium Welds Made with Different Shielding Conditions (a)

Thickness (in.)	Shield Gas	HAZ Color	Weld Color
0.079 (2 mm)	100% Argon	Silver	Silver
0.079 (2 mm)	HP-Argon(b)	Silver	Silver
0.079 (2 mm)	0.21% Air	Silver/Some Straw	Silver
0.079 (2 mm)	0.21% Air	Dark Blue/Some Straw	Silver
0.079 (2 mm)	0.43% Air	Silver	Silver
0.079 (2 mm)	0.43% Air	Silver/Some Straw	Silver
0.079 (2 mm)	0.60% Air	Straw/Dark Blue	Silver
0.079 (2 mm)	0.60% Air	Straw/Dark Blue	Silver/Straw
0.079 (2 mm)	0.60% Air	Straw/Dark Blue	Straw
0.079 (2 mm)	0.79% Air	Straw/Dark Blue	Silver/Some Straw
0.079 (2 mm)	0.79% Air	Straw/Dark Blue	Silver/Some Straw
0.079 (2 mm)	0.97% Air	Straw/Dark Blue	Silver/Some Straw
0.079 (2 mm)	0.97% Air	Straw/Dark Blue	Silver/Some Straw
0.079 (2 mm)	HP-Argon (No. 12 Cup)(c)	Blues	Light Blue/Burgundy
0.079 (2 mm)	HP-Argon (No. 12 Cup)(c)	Blues	Light Blue/Burgundy
0.079 (2 mm)	HP-Argon (No. 8 Cup)(c)	Burgundy/Blues	Burgundy
0.079 (2 mm)	HP-Argon (No. 8 Cup)(c)	Burgundy/Blues	Burgundy

(a) All welds were made at 3.5 in./min travel speed, 11°C/s cooling rate.
(b) HP-Argon = high-purity Argon ≥ 99.998% pure by volume, 100% Argon ≥ 99.985% pure by volume.
(c) An argon gas trail shield was not used to protect the cooling weld bead after solidification; trail shield length = 3 in. (76.2 mm).

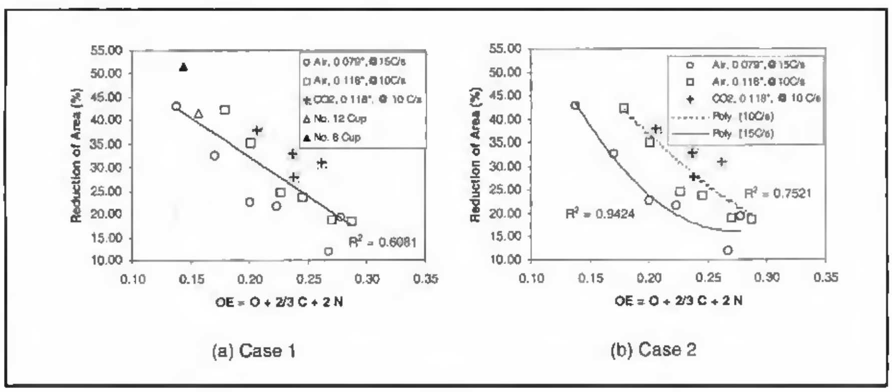

Fig. 7 — OE_{CP} effects on longitudinal tensile reduction of area.

the same solution or performance in fitting the regression model. Besides, it was more conventional to let other C varies as the proportion of oxygen coefficient while keeping the oxygen coefficient to the value of 1. Solving the above problem yielded the oxygen equivalent coefficient matrix, C.

Results and Discussion

Weld Color Observations

The color of the titanium weld varied between tests depending on the welding parameters, sheet thickness and alloy type (CP or Ti-6AL-4V). Welds made using contaminated torch shielding gas used pure argon backing and trailing shields to protect the molten metal from further contamination. As a result, welds made on the 0.079-in. (2.0-mm) CP Grade 2 titanium using air-argon torch shielding gases of up to 0.60% air were essentially silver — Table 5. Straw-colored welds were made with the 0.79 and 0.97% air-argon shielding gases. The HAZ color changed through a spectrum of colors from silver to straw to dark blue as the air content of the torch shielding gas increased from zero to 0.43% to 0.97%, respectively. The weld color of the autogenous welds made on the 0.118-in. (3.0-mm) CP Grade 2 titanium was straw or darker because the 3-in. (76.2-mm) long trailing shield was too short to provide complete trailing gas coverage during cooling of the thicker section, which was also welded at a higher travel speed. The same problem was observed on the two thicknesses of Ti-6Al-4V. The operator witnessed the color change as the hot weld metal left the protection of the trailing shield.

The color of titanium welds is related to the oxidizing conditions of the torch and trailing shield during welding, the peak temperature and the weld metal cooling rate. Higher air contents in the shielding gas were more likely to contaminate the trailing shield gas and promote darker weld colors. Slower cooling rates also promoted darker colors since the weld metal was at higher oxidation temperatures as it left the protection of the argon trailing shield. The silver welds produced with air-argon shielding gases were probably a result of the weld pool absorbing the majority of the air contaminates and the slower weld travel speed, which permitted cooling below the oxidation temperature range before the weld metal left the protection of the trailing shield. Therefore, a silver weld can be contaminated when the majority of the contamination is absorbed by the weld pool area at very high temperatures, any surface oxides that form are dissolved into the subsurface, and the trailing shield is long enough to assure argon coverage to weld metal temperatures below 840°F (449°C). However, the weld craters of the welds made with air-contaminated shielding gases were discolored due to prolonged exposure during torch shielding postpurge. In addition, the tungsten electrodes were degraded by the contaminated shielding gases. Oxide whiskers grew on the end of the electrodes and the size of the whiskers increased with increasing air or CO_2 content in the torch shielding gas.

Autogenous welds also were made on the 0.079-in. (2.0-mm) thick CP titanium with just a No. 8 and a No. 12 cup using HP argon and no trailing shield. Table 5 shows these welds were very discolored. The weld face color of the No. 8 cup test was burgundy. The HAZ color was a rainbow of color where the far HAZ was straw and the color sequence went from burgundy to blues to silver hiatus (Ref. 8) and then repeated the sequence near the weld interface. The weld crater and adjacent material on these welds were silver from the shielding gas postpurge, indicating adequate gas shielding over the weld pool area. Therefore, the color seen on the No. 8 and No. 12 cup welds was primarily due to surface oxides that formed after solidification.

CP Titanium Weld Properties

Transverse tensile tests were initially performed on the autogenous 0.079-in. (2-mm) thick welds, but the results did not relate to the effects of air contamination since all of the specimens broke in the softer HAZ where grain coarsening had occurred. The ultimate strength of these transverse tests varied from 56.7 to 63.0 ksi (390.9 to 434.4 MPa). This was slightly less than the base metal ultimate strength, which averaged near 70 ksi (482.6 MPa) but was greater than the ASTM requirements of 50 ksi (344.7 MPa) for Grade 2 — Table 1.

Longitudinal tensile tests provided a better measurement of weld metal strength (Figs. 4 and 5) and ductility (Figs. 6 and 7). An autogenous weld made at 15°C/s cooling rate with 0.97% air-argon torch shield had the highest strength and lowest ductility. The properties were 73.0 ksi (503.3 MPa) yield strength, 81.0 ksi (558.5 MPa) ultimate strength, 9.2% elongation and 19.3% RA. Welds made with high-purity argon had the lowest strength and highest ductility. The range of tensile properties for these welds was 53 to 56 ksi (365.4 to 386.1 MPa) yield strength, 63 to 66 ksi (434.4 to 455.0 MPa) ultimate strength, 29 to 31% elongation and 42 to 43% RA.

Welds made without trailing shields using just the No. 12 or No. 8 cup had essentially the same tensile properties as welds made with high-purity argon. It appeared the oxide and alpha-case layers on the No. 12 and No. 8 cup test welds, which were left in the as-welded condition, were not thick enough to affect tensile properties. Table 3 confirms the composition of these welds was essentially the same as welds made with high-purity argon and an argon trailing shield. The properties exceeded ASTM requirements for Grade 2 base material — Table 1.

Oxygen equivalents for welds made with high-purity argon shielding gas varied from 0.141 to 0.181 wt-% for the 0.079- and 0.118-in. (2- and 3-mm) thicknesses, respectively. The latter material heat had a higher as-received oxygen content and strength. The OE of the No.

Table 6 — Average 95% Confidence Intervals (+, –) for Data Points from Weld Property Tests

Property	Commercially Pure Titanium 0.079-in. (2-mm) thick	Commercially Pure Titanium 0.118-in. (3-mm) thick	Titanium 6Al-4V 0.080-in. (2.03-mm) thick	Titanium 6Al-4V 0.125-in. (3.17-mm) thick
Yield (ksi)	1.21	1.54	3.23	3.30
Ultimate(ksi)	1.49	1.26	3.24	2.70
Elongation (%)	2.24	4.57	1.29	1.00
ROA (%)	6.66	9.22	3.81	4.44
Rockwell	1.19 (R_B)	1.62 (R_B)	1.11 (R_C)	1.43 (R_C)
Vickers (VHN)	7.65	9.21	7.97	9.70

Table 7 — R^2 Comparison of OE Relationships

	CP Ti Case 1	CP Ti Case 2 f(cooling rate)	Ti-6Al-4V OE = 20.8C + 7.8N + 0 – 5.8 Fe
Yield Strength	0.7842	0.9943 (15 c/s) 0.8451 (10 c/s)	0.507
Ultimate Strength	0.8751	0.9978 (15 c/s) 0.8126 (10 c/s)	0.2843
Elongation	0.5722	0.9764 (15 c/s) 0.7107 (10 c/s)	0.4882
Reduction of Area	0.6081	0.9424 (15 c/s) 0.7521 (10 c/s)	0.1474
Rockwell B/C	0.8804	0.9949 (15 c/s) 0.8198 (10 c/s)	0.403
Vickers	0.8817	0.9754 (15 c/s) 0.8665 (10 c/s)	0.5023
Average R^2	0.7602	0.8898	0.3887

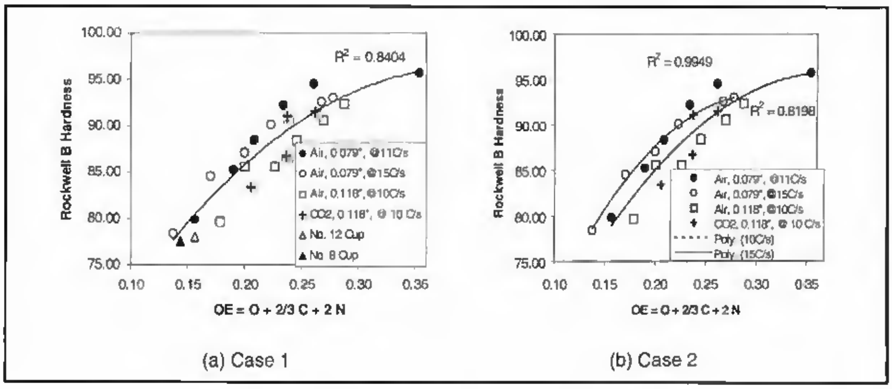

Fig. 8 — OE_{CP} effects on weld face hardness (Rockwell B).

8 and No. 12 weld tests, which were made on the 0.079-in. titanium, was 0.149 and 0.156 wt-%, respectively. It was concluded no appreciable contamination occurred in the welds made without trailing shields because mechanized GTAW was employed under very controlled conditions where proper torch shielding protected the weld pool.

Longitudinal weld metal tensile results for CP titanium welds were compared to the oxygen equivalent equation, OE = 2/3C + O + 2N. As expected, strength increased (Figs. 4 and 5) and ductility decreased (Figs. 6 and 7) as the oxygen equivalent increased for CP titanium welds. In each of these figures, the data is graphed two ways: a best fit of all the data (Case 1) and two curves to fit data as a function of cooling rate (Case 2). The two case approach to analysis was used to determine if weld metal cooling rate over a range from 10 to 15°C/s had an effect on properties. The cooling rate between 800 to 500°C (1472 to 932°F) was determined to be approximately 10 and 15°C/s for the 0.118- and 0.079-in. (3- and 2-mm) welds, respectively. These cooling rates are representative of manual GTA welds.

Ultimate strength (Fig. 4) varied from 63 to 81 ksi (434.4 to 558.5 MPa) over the

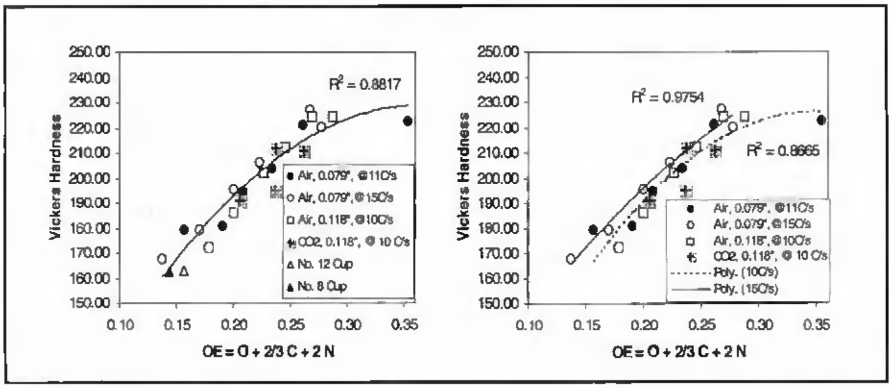

Fig. 9 — OE_{CP} effects on weld microhardness.

OE range of 0.14 to 0.30 wt-%. For ultimate strength, the coefficient of multiple determinations (R^2) was determined to be 0.87 for Case 1 and 0.99 and 0.81 for Case 2 cooling rate curves. The Case 2 analysis did not show significant benefit for improving the relationship between OE and ultimate strength since the Case 1 R^2 value was sufficiently high.

The Case 2 relationship was stronger when evaluating the other CP titanium weld properties, like weld metal yield strength as shown in Fig. 5. Here the R^2 was 0.78 for Case 1 and 0.99 and 0.85 for Case 2. The yield strength ranged from 53 to 73 ksi (365.4 to 503.3 MPa) over the oxygen equivalent range. A cooling rate effect was observed where the slower cooling 0.118-in. (3-mm) thick welds had a yield strength approximately 4 ksi (34.5 MPa) lower than the 0.079-in. (2-mm) thick welds as a function of oxygen equivalent — Fig. 5.

The relationship between oxygen equivalent and tensile ductility was dependent on cooling rate for the CP titanium welds (Figs. 6 and 7). In general, weld ductility decreased as the oxygen equivalent increased for CP titanium welds. Elongation ranged from 31% to 8% over the OE range of 0.14 to 0.30 wt-%, respectively. Reduction in area ranged from 43% to 10% over the same OE range. The OE_{CP} formula produced a good trend for both elongation and reduction of area for the Case 2 analysis where the R^2 values for elongation were 0.57 for Case 1 and 0.98 and 0.71 for Case 2 cooling rates. The welds made with the lower cooling rate (10°C/s) had approximately 7% more elongation and 10% more reduction in area than welds made at comparable oxygen equivalents at the higher cooling rate.

Most CP titanium welding applications require the weld ductility to be greater than 12% to 20% elongation depending on the application. Based on the welds made here, the minimum OE corresponding to these ductility levels would be approximately 0.24 to 0.18 wt-%, respectively. The latter oxygen equivalent was equal to the oxygen equivalent of the 0.118-in. (3-mm) CP base metal. Therefore, care should be exercised when procuring CP titanium when high ductility is required in the weld metal. Since oxygen has been reported to affect toughness, especially at cryogenic temperatures, the effects of oxygen equivalent on toughness and corrosion resistance is another area for future work.

The tensile ductility of the single-pass welds made without trailing shields was essentially the same as the welds made with trailing shields using proper torch argon shielding. These tests were conducted with the alpha case left in the as-welded condition. Even though the tensile ductility of these tests was acceptable, mixed results were obtained in a prior investigation of bend tests (Ref. 1) that were performed on as-welded longitudinal test specimens. In this investigation, bend tests performed at 2T bend radii (20% strain) passed, but one of four bend tests performed at 4T bend radii (12% strain) failed due to two small cracks that formed on one side of the weld interface. This bend failure was hard to explain, but reinforces the risk a fabricator would take if welds are put in service with thick oxide and alpha case. Based on previous bend test results on single-pass welds, it did appear that some thickness of oxide and alpha case could be tolerated before bend ductility is unacceptable. The effects of oxide and alpha case on fatigue performance may be more severe and is another area that needs to be quantified for weldments. The alpha case that formed on the CP titanium welds made without trailing shields was not obvious in metallographic cross sections.

Rockwell B hardness measurements were made on the weld face and root on each welding test so data generated here could support the use of portable hardness testers that are being considered for weld inspection. The difference in hardness between the weld face and root was small but, in general, the weld face was slightly harder. This indicated the contamination introduced into the weld pool was mixed through the weld thickness. The weld face probably had a slightly higher concentration of interstitial elements. The weld face Rockwell B hardness (Fig. 8) averaged about 78 R_B for the single-pass welds made with high-purity argon shielding gas with or without a trailing shield. The 0.079-in. (2-mm) thick base material used on these tests had a hardness of approximately 81.5 R_B. The 0.118-in. (3-mm) thick base material had a hardness that averaged 86 R_B. The cast grain structure of the weld metal was believed to cause the lower hardness between the weld metals and base materials, which were wrought. Hardness measurements on the HAZ were always lower than the base metal due to grain coarsening of the single-phase HCP alpha.

Weld metal Rockwell B hardness increased as the oxygen equivalent increased for these autogenous welds — Fig. 8. The hardness ranged from 78 to 95 R_B over an OE range of 0.14 to 0.35 wt-%, respectively. The 0.079-in. (2-mm) thick welds made with 0.97% air (0.354 oxygen equivalent) had the highest macrohardness of approximately 95 R_B. The 0.118-in. (3-mm) thick welds were approximately 2 R_B softer than the 0.079-in. (2-mm) thick welds as a function of oxygen equivalent due to the lower cooling rate. The cooling rate effect did not appear to be as strong for Rockwell B hardness. The R^2 values for the curves shown in this figure was 0.84 for Case 1, and was 0.99 at 15°C/s and 0.82 at 10°C/s for the Case 2 cooling rates.

AWS D10.6-91 notes that a satisfactory weld should have a hardness that does not exceed the base metal hardness by 5 R_B (which is equivalent to about 30 H_V) and peak hardness should not exceed 100 R_B. The macrohardness of the 0.079-in. (2-mm) thick base material in this investigation averaged about 81.5 R_B. Based on AWS recommendations, welds with a hardness of up to 86.5 R_B with an oxygen equivalent of 0.20 wt-% should be acceptable. This oxygen equivalent correlated to approximately 16% elongation, which should be acceptable on applications with a 4T bend criteria. Likewise, a hardness of 91 R_B should be acceptable for the 0.118-in. (3-mm) thick material based on the +5 R_B rule. This

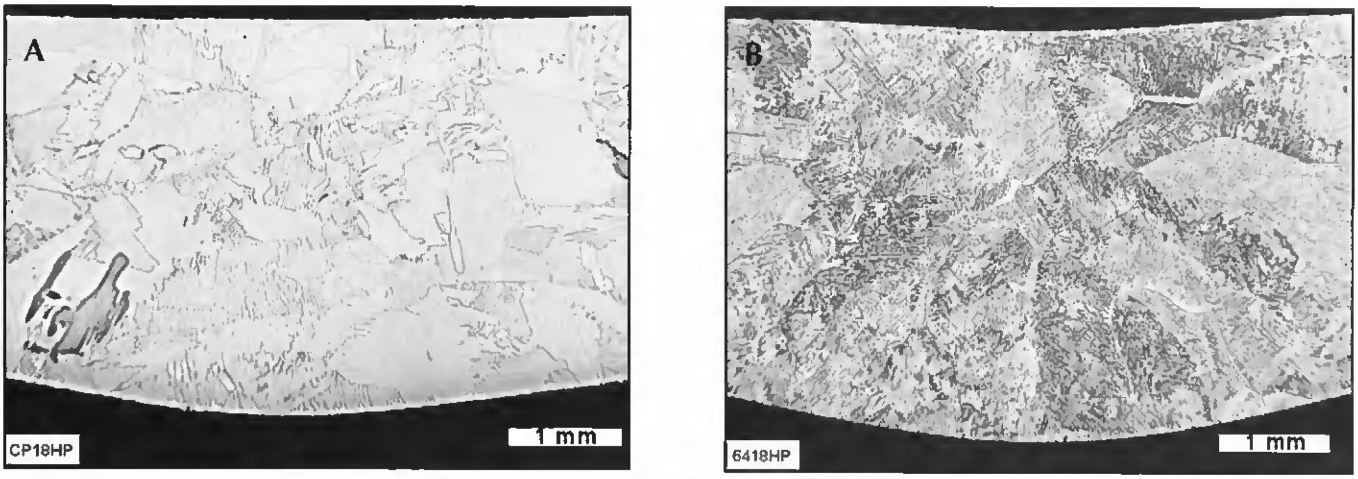

Fig. 10 — Macrostructure of autogenous welds. A — Serrated Alpha in CP titanium; B — Acicular Alpha and Beta with Alpha on prior Beta grain boundaries in Ti-6Al-4V.

hardness correlated to an oxygen equivalent of 0.30 wt-% and an elongation of 10%. Based on the results here, the +5 R_B rule provided as a recommendation in AWS D10.6-91 will be sensitive to the starting composition of the base material, the contamination absorbed during welding and the weld cooling rate. The rule should probably be used with caution depending on interstitial content of the base material and the ductility required on the welding application.

Vickers microhardness measurements (Fig. 9) were made on a metallographic cross section from each CP titanium weld. Microhardness averaged less than 165 H_V for the welds made with high-purity argon shielding both with and without trailing shields. For the welds made with contaminated shielding gas, the microhardness increased as the oxygen equivalent of the weld metal increased to a maximum of 225 H_V at 0.29 wt-%. The 0.118-in. (3-mm) thick welds had a microhardness that was approximately 5 H_V lower than the 0.079-in. (2-mm) thick welds as a function of oxygen equivalent due to the lower cooling rate. The R^2 value for the curves shown in Fig. 9 was 0.88 for Case 1, and was 0.98 at 15°C/s and 0.87 at 10°C/s for the Case 2 cooling rates. As with Rockwell B hardness, the effects of cooling rate on Vickers hardness was not as great as for tensile strength or ductility.

The average 95% confidence level band was calculated for each data point on Figs. 4 through 9, as shown in Table 6. For Vickers hardness, the average variation in a group of measurements was ±7.5 H_V. Microhardness testing required an average of at least six to nine intragranular measurements to account for the scatter caused by grain orientation. A bimodal hardness distribution was typically observed on Vickers hardness data and was believed to be due to the anisotropic mechanical behavior of alpha HCP titanium. The operator believed this hardness distribution could be correlated to the etching of the sample (*i.e.*, light vs. dark etching grains). Based on these results, an average of a large group of microhardness measurements is recommended when assessing the hardness of titanium welds.

Overall, the oxygen equivalent formula produced a uniform relationship for most of the weld metal test conditions evaluated in this investigation for CP titanium. A comparison of R^2 values between Case 1 (which evaluated a direct relationship to the OE) and Case 2 (which evaluated an indirect relationship to OE as a function of cooling rate) was performed as shown in Table 7. The average R^2 value calculated by averaging the sum of all the individual R^2 calculations was 0.76 for Case 1. This was significantly lower than 0.89 for Case 2, which factored the effects of cooling rate. Based on this analysis, it appeared CP titanium weld properties were sensitive to cooling rate. Most of the variability observed in the Case 2 analysis was from the tests performed at 10°C/s cooling rate on the 0.118-in. (3-mm) material where both air-argon and CO_2-argon contamination was evaluated. This additional variability could be attributed to either the accuracy of the OE equation to account for the interactive effects of each interstitial element, carbon, oxygen and nitrogen; or the effects of iron additions that varied from 0.03 to 0.06 wt-% between the two heats of CP titanium material that was evaluated here. Future work should perform a more systematic evaluation of the factors that control properties in CP titanium welds. These factors should include interstitial and iron content, and weld metal cooling rate based on this investigation.

Metallographic analysis of the CP titanium test welds was performed to characterize any differences in microstructure due to air or CO_2 contamination. In general, the welds had a serrated alpha grain structure — Fig. 10. Some areas had some Widmanstätten structures. The Widmanstätten structure is reported to become more dominant in CP titanium as the oxygen and nitrogen content increase (Refs. 2, 3). The intragranular areas had a platelike substructure where the interplate boundaries are probably rich in iron and may have some beta phase present. The iron content was low, approximately 0.03 and 0.06 wt-% in the 0.118- and 0.079-in. (3- and 2-mm) materials, respectively. The low iron content of these heats would probably provide enhanced corrosion resistance and toughness. Iron is considered a solid-solution strengthener in CP titanium. Heats too low in iron are possibly more susceptible to hydride precipitation (Ref. 11). Hydrides have been observed to precipitate in commercial heats containing iron near 0.3 wt-% at hydrogen levels near 100 to 150 ppm. High-purity titanium was found to precipitate hydrides at 40 ppm hydrogen (Ref. 11). No hydride needles were observed in these metallographic cross sections and the welds made here typically had less than 20 ppm hydrogen. No differences were observed in substructure due to differences in carbon, nitrogen or oxygen content under optical metallographic examination.

Ti-6Al-4V Weld Properties

Several differences were observed when comparing the welding characteristics and weld properties of CP titanium and Ti-6Al-4V. The first difference was there were almost no changes in weld metal cooling rate in the Ti-6Al-4V welds

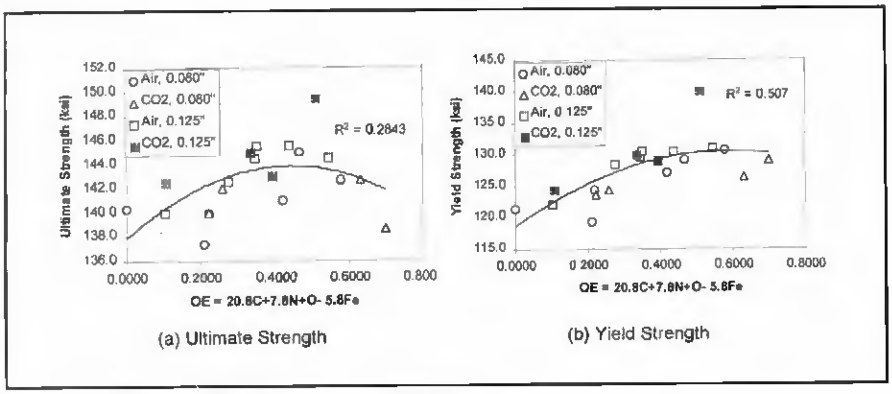

Fig. 11 — $OE_{Ti\text{-}6Al\text{-}4V}$ effects on longitudinal weld strength.

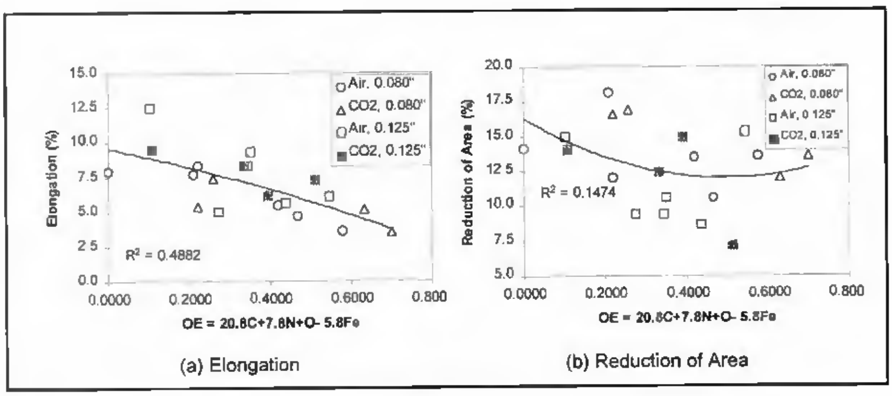

Fig. 12 — $OE_{Ti\text{-}6Al\text{-}4V}$ effects on weld ductility.

due to welding different thickness materials. In CP titanium, the cooling rate was either 15 or 10°C/s for full-penetration welds that had a ¼-in. (6.35-mm) root bead width at 7.75 in./min (3.28 mm/s) travel speed as the thickness was changed from 0.079- to 0.0118 in. (2 to 3 mm), respectively. For Ti-6Al-4V full-penetration welds with ¼-in. (6.35-mm) root bead width, there was only a slight variation in cooling rate for the two thicknesses of materials, 0.080 and 0.125 in. (2.03 and 3.17 mm), that were evaluated. The 0.080-in. (2.03-mm) material was welded at 8.5 in./min (3.6 mm/s) travel speed and the weld metal cooling rate between 800 and 500°C (1472 and 932°F) was 12.5°C/s. For the 0.125-in. (3.18-mm) material welded at 9.0 in./min (3.81 mm/s) travel speed, the cooling rate was 11.8°C/s. The low thermal conductivity of Ti-6Al-4V was believed to nullify the effects of thickness on the tests performed here. The backing fixture used in this investigation had a 2-in. (50.8-mm) wide gap to minimize tooling effects and simulate non-backed welding applications. Therefore, for this investigation the effect of cooling rate on Ti-6Al-4V weld properties was considered negligible and was not related to the oxygen equivalent. Literature suggests the effects of cooling rate are much stronger in Ti-6Al-4V compared to CP titanium due to the solid-state phase transformation that occurs with changes in cooling rate. Future investigations may consider comparing different weld processes to produce stronger changes in weld metal cooling rate, use materials with greater thickness differences, or force cool the weld metal to study cooling rate effects on OE relationships.

The second observation was that a new OE equation needed to be developed for Ti-6Al-4V weld metals to better relate the factors that affect weld properties. The Ti-6Al-4V weld metal properties measured here were first related to the oxygen equivalent equation that was used for CP titanium, $OE_{CP} = 2/3C + O + 2N$, but the data fit was poor and unacceptable. In general, the welds contaminated with carbon and oxygen (from CO_2-argon contamination) were observed to have higher strength and hardness and lower ductility than welds made using air-argon contamination at the same relative OE_{CP} level. It was apparent carbon was a more potent strengthener in Ti-6Al-4V than in CP titanium. A statistical regression analysis was performed to derive a new oxygen equivalent formula to best fit the Ti-6Al-4V data. The new OE equation was determined by maximizing the R^2 value for each weld metal property and was the following:

$$OE_{Ti\text{-}6Al\text{-}4V} = 20.8C + 7.8N + O - 5.8Fe \text{ (wt-\%)}$$

This equation indicates carbon has 20.8 times the effect on weld metal properties as does oxygen. Nitrogen is 7.8 times and iron is negative 5.8 times more potent than oxygen. Due to the larger factors, the oxygen equivalent range calculated by this equation is much larger than produced by the OE_{CP} equation. The most significant change relative to the OE_{CP} equation is the increase in the carbon factor from 2/3 to 20.8. Nitrogen was increased from 2 to 7.8 and a factor was added for iron, which has a negative effect. Iron was not measured in the composition analysis of each weld metal test. The iron factor was determined by assuming constant base metal content for each material heat per the levels shown in Table 1. The maximized R^2_{AVG} was 0.39 and was calculated by averaging the R^2 values for each property shown in Table 7. This was considered a weak fit overall and indicated the oxygen equivalent relationships for Ti-6Al-4V, based on interstitial content, do not work since these elements had such a small effect on strength, hardness and ductility. Other factors that were not controlled in these tests, such as the actual iron, aluminum and vanadium content, and prior beta grain size (Ref. 15), may need to be studied to properly characterize all the factors that affect Ti-6Al-4V weld metal properties.

Even though correlation was poor for the relationships measured, there were small trends between $OE_{Ti\text{-}6Al\text{-}4V}$ and the different weld properties. The relationship between $OE_{Ti\text{-}6Al\text{-}4V}$ and tensile strength (Fig. 11), tensile ductility (Fig. 12) and hardness (Fig. 13) were graphed for analysis. The relationship between ultimate strength and $OE_{Ti\text{-}6Al\text{-}4V}$ was fairly weak as shown in Fig. 11A where the R^2 value was only 0.28. The ultimate strength of the cast weld metal varied from 137 to 146 ksi (944.6 to 1006.7 MPa) over an OE range of 0.10 to 0.70 wt-%. Ultimate strength slowly increased with increasing OE but appeared to slightly decrease at $OE_{Ti\text{-}6Al\text{-}4V}$ greater than 0.50 wt-%.

The Ti-6Al-4V oxygen equivalent relationship was slightly better for weld metal yield strength (Fig. 11B) where the R^2 value increased to 0.51. Yield strength increased as the oxygen equivalent increased as expected. The yield strength varied from 120 to 130 ksi (827.4 to 896.3 MPa) as the oxygen equivalent increased from 0.10 to 0.70 wt-%. No difference in yield strength was observed between the 0.080- and 0.125-in. (2.03- and 3.17-mm) thicknesses of material since the welds had approximately the same cooling rate. Weld metal yield strength was lower than the base materials when comparing the weld properties from the high-purity argon shielding tests. The yield strength of the base material was 132 and 140 ksi (910.1 and 965.3 MPa) for the 0.080- and 0.125-in. (2.03- and 3.17-mm) thicknesses, respectively. The heat treatment condition for the 0.125-in. (3.17-mm) Ti-6Al-4V sheet was not reported. The 0.080-in. (2.03-mm) base metal was supplied in the annealed condition where the heat treatment parameters were 770°C (1418°F) for 10 minutes then air-cooled.

Weld metal elongation decreased with increasing oxygen equivalent — Fig. 12A. The weld metal elongation varied from approximately 10 to 4% as the oxygen equivalent increased from 0.10 to 0.70 wt-%. The R^2 value for the curve in this graph was 0.49, which again indicated the relationship was weak. The high-purity argon shielding test had the highest elongation of 12.5%. The lowest elongation was 4% and was produced using the 1.0% CO_2-argon shielding gas. Tensile ductility measurements on Ti-6Al-4V welds were believed to be sensitive to the coarse-grain structure, which can behave anisotropically, and the limited ductility of the high strength Ti-6AL-4V weld metals. The data fit was worse for reduction of area (RA) (Fig. 12B) where the R^2 value decreased to 0.15, indicating a poorer relationship. The high-purity shielding gas tests averaged between 14 and 15% RA at $OE_{Ti\text{-}6Al\text{-}4V}$ values of approximately 0.1 wt-%. At higher $OE_{Ti\text{-}6Al\text{-}4V}$ values greater than 0.20 wt-%, the RA ranged from 8 to 15% and showed almost no relationship to OE.

Rockwell C hardness measurements were made on the weld face of each test weld — Fig. 13. Hardness increased from approximately 30 to 36 Rockwell C over the range of oxygen equivalents tested. This was a small hardness range and showed the hardness of this titanium alloy was more dependent on microstructure than interstitial content. The 95% confidence level for this data (Table 6) was about the same as the CP titanium data, but there was more variation as a function of oxygen equivalent. The R^2 value for curve in Fig. 13A was 0.40. The hardness of the welds made with high-purity argon was 30 to 32 R_C. The same trend was found in Fig. 13B, which shows the Vickers hardness data where the R^2 value was 0.50. The Vickers hardness ranged from 327 to 358 over the $OE_{Ti\text{-}6Al\text{-}4V}$ range. Welds made with high-purity argon had a Vickers weld metal hardness of 332 to 335. The limited range of hardness in the Ti-6Al-4V welds is closely related to the range of ultimate strength, which was also small in this high-strength material over the range of compositions evaluated here. The use of hardness testing to assess the quality level of Ti-6Al-4V welds appears not feasible, based on the variance in data.

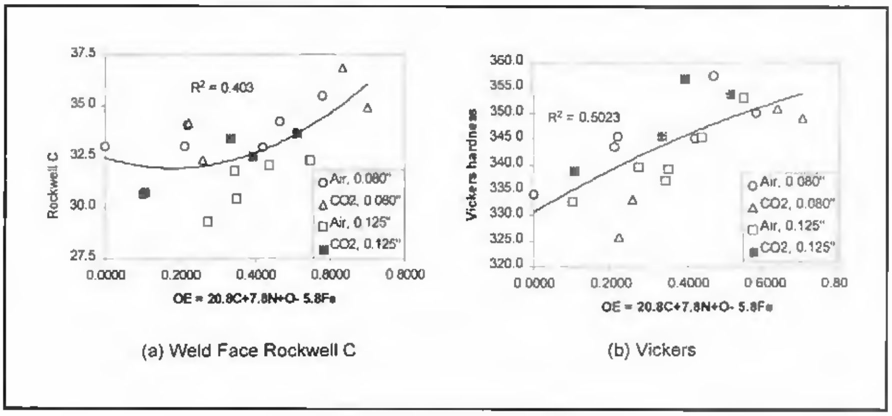

Fig. 13 — $OE_{Ti\text{-}6Al\text{-}4V}$ effects on weld hardness.

Metallographic analysis of the Ti-6Al-4V test welds was performed to characterize any differences in microstructure due to air or CO_2 contamination. In general, all the welds had acicular alpha and beta substructure with alpha on prior beta grain boundaries — Fig. 10. This microstructure was not believed to contain any alpha prime, which is a martensitic transformation product. These welds had a low cooling rate of about 12°C/s, so the transformations should have been due to nucleation and growth processes. Hydrides are difficult to form in Ti-6Al-4V due to the high content of beta stabilizers and are not likely in these microstructures due to their low hydrogen content.

Overall, Ti-6Al-4V is a high-strength material that has low to moderate ductility. The high strength can be related to its high hardness. The properties of Ti-6Al-4V welds are largely influenced by prior beta grain size, microstructure, solid-solution strengthening primarily by aluminum, and by second phase effects induced through transformations. It appears from the data measured here interstitial strengthening had a small effect and minimizes the benefit of using oxygen equivalent relationships. Future work is needed to better characterize all the factors that control the properties of Ti-6AL-4V weld metal.

Conclusions

1. Oxygen equivalent formulas were used to relate weld metal mechanical properties to interstitial content and cooling rate for CP titanium. The mechanical property relationships that were characterized for CP titanium appeared to be dependent on weld metal cooling rate.

2. Macrohardness (Rockwell B) testing can be used to correlate weld face hardness of CP titanium to other weld mechanical properties and interstitial content via the oxygen equivalent formula, and could be used to assess for contamination. A hardness standard as a function of oxygen equivalent should be developed for each weld application and cooling rate.

3. The oxygen equivalent equation developed for Ti-6Al-4V could not be used to relate the effects of interstitial elements on weld metal properties.

Acknowledgments

EWI funded this investigation through its cooperative research and development program. Members of the aerospace, heavy manufacturing and energy and chemical industry advisory committee are acknowledged for supporting this program. Jack Moore, former part-time student intern, is acknowledged for his efforts helping in the lab and graphing data. Harry Pulsifer, Rock Island Arsenal, and Martin Wells, Army Research Laboratory, are acknowledged for donating Ti-6Al-4V base material to this investigation.

References

1. Harwig, D. D., and Castner, H. 1996. Oxygen equivalent effects on the mechanical properties of titanium welds. *The International Conference on Advances in Welding Technol-*

ogy, Columbus, Ohio.

2. *TITANIUM — A Technical Guide.* 1989. Edited by M. J. Donachie, ASM International.

3. Martin, D. C. 1953. Effects of carbon, oxygen and nitrogen on welds in titanium. *Welding Journal* 32: 139-s to 154-s.

4. Barrett, *et al.* 1953. Effect of atmospheric contaminants on arc welds in titanium. *Welding Journal* 32(6): 283-s to 291-s.

5. Hartbower, *et al.* 1954. Alloy welds deposited in unalloyed titanium base metal: Part 2. *Welding Journal* 33(8): 408-s to 415-s.

6. Morgan-Warren, E. J. 1978. Atmospheric control criteria for welding titanium. *Proceedings from Advances in Welding Processes*, Paper 10.

7. Raja, *et al.* 1979. Open air welding of commercially pure titanium. *Indian Welding Journal* (7): 79–83.

8. Gittos, M. F., Scott, M. H., and Nicholson, R. J. K. 1980. Effect of contamination by air on the TIG welding of commercially pure titanium sheet. TWI Research Report No. 115/1980.

9. Heikinheimo, *et al.* 1991. Increasing productivity in welding of titanium with high quality requirements. *Int. J for the Joining of Materials* 3(2).

10. Ogden, H. R., and Jaffee, R. L. 1955. The effects of carbon, oxygen, and nitrogen on the mechanical properties of titanium and titanium alloys. Battelle Memorial Institute, TML Report No. 20.

11. *ASM Handbook.* 1994. Vol. 6, Welding, brazing, and soldering, p. 512.

12. Lenning, G. A., Craighead, C. M., and Jaffee, R. I. 1954. Constitution and mechanical properties of titanium-hydrogen alloys. *AIME, Journal of Metals*, Vol. 200.

13. Gould, J. E., Becker, D., and Williams, J. C. 1980. Microstructural characterization of Ti weldments. *Proceedings of Physical Metallurgy of Metal Joining.* AIME Fall Meeting, St. Louis, Mo.

14. Mitchell, D. R. 1965. Porosity in titanium welds. *Welding Journal* 44(4): 157-s to 167-s.

15. Inoue, H., and Ogawa, T. 1989. Effect of weld cooling rate on the microstructure and properties of Ti-6Al-4V weldment. *Proceedings from Evaluation of Materials Performance in Severe Environments*, EVALMAT 89, Kobe, Japan.

16. Murthy, K.K. and Sundaresan, S. 1995. Microstructure and tensile properties of the fusion zone in Ti-6Al-4V weldments. *International Journal for the Joining of Materials* 7(4).

17. Kivineva, E., Hannerz, N. E., and Sjoberg, R. 1995. Microstructure of Ti-6Al-4V weld metal and simulated HAZ. *Proceedings from OMAE*, Vol. III, Materials Engineering.

18. Kosaka, Y., *et al.* 1998. The effect of welded microstructure on ballistic properties of Ti-6Al-4V plates. *Proceedings from Non-Aerospace Applications of Titanium.* The Minerals, Metals and Materials Society.

19. Murthy, K. K., Potluri, N. B., and Sundaresan, S. 1997. Fusion zone microstructure and fatigue crack growth behavior in Ti-6Al-4V alloy weldments. *Materials Science and Technology*, Vol. 13.

20. Boucher, C., *et al.* 1994. Open-air welding of medium thickness TA6V titanium alloy. *EUROJOIN* 2, Florence 16/18.

21. Imam, M. A., Judy, R. W., and Rath, B. B. 1987. Evaluation of tensile flow properties of weldments in titanium alloys. *Welding Journal* 66(7): 210–214.

22. Radhakrishna, Ch., Reddy, J. R., and Rao, K. P. 1997. Study on microstructures of electron beam and gas tungsten arc Ti-6Al-4V weld metals. *Prakt. Metallogr.* 34:4.

23. Venkataraman, G., and Mitra, T. K. 1994. A new method of studying weld metal microstructures of Ti-6Al-4V without polishing. *National Welding Seminar '94.*

24. Murthy, K. K., and Sundaresan, S. 1997. Fracture toughness of Ti-6Al-4V after welding and post-weld heat treatment. *Welding Journal* 76(2): 81-s to 92-s.

25. Thomas, G., *et al.* 1992. Effect of pre-weld and post-weld heat treatment on the properties of GTA welds in Ti-6Al-4V sheet. *Welding Journal* 71(1): 15-s to 20-s.

26. Radhakrishna, Ch. and Rao, K. P. 1997. Comparative study on impact toughness of gas tungsten arc and electron beam weld metals of Ti-6Al-4V. *Materials Science and Technology*, Vol. 13., pp. 1057–1062.

27. Borggreen, K. and Wilson, I. 1980. Use of post-weld heat treatments to improve ductility in thin sheets of Ti-6Al-4V. *Welding Journal*, 59(1): 1-s to 9-s.

28. Enjo, T., Kuroda, T., and Nishizawa, M. 1988. Microstructure and mechanical properties in heat affected zone of titanium alloy. *Transactions of JWRE*, Vol. 17, no. 2.

29. Shah, A. K., *et al.* Oct. 1995. Weld heat affected zone in Ti-6Al-4V alloy, Part II — Modeling and experimental simulation of growth and phase transformations. *Welding Journal* 325-s to 378-s.

30. Okazakij, K., and Conrad, H. 1973. Effect of grain wize and interstitial solute content on the hardness of Ti-N, Ti-O, and Ti-C alloys at room temperature, *Transcript of JIM*, Vol. 14.

31. *Design and Analysis of Experiments*, 1996. D.C. Montgomery, John Wiley and Sons Inc., 4th edition.